DOI 10.1007/s11182-022-02588-3
Russian Physics Journal, Vol. 64, No. 12, April, 2022 (Russian Original No. 12, December, 2021)

OPTICS AND SPECTROSCOPY

TRANSMISSION OF OPTICAL RADIATION BY A POLYDISPERSE ICE CLOUD

O. V. Shefer[1] and O. K. Voitsekhovskaya[2] UDC 535.36:551.510

Results of calculation of the transmission function for ensembles of ice crystals typical of crystal clouds are presented as functions of the wave numbers. Considering different shapes, size spectra, and aspect ratios of randomly and predominantly oriented crystal ensembles, the transmission function is analyzed in the wavelength range from 0.5 to 15 μm. The most clearly expressed spectral features of the transmission function attendant to variations in the physical and chemical parameters of particles have been noted for large horizontally oriented plates. The influence of different particle sizes and concentrations on the transparency of the medium has been estimated.

Keywords: transmission, optical radiation, ice clouds, crystals, orientation.

INTRODUCTION

Crystal clouds play an important role in the weather-forming processes in the Earth atmosphere. International experts on the problem "Climatic changes" claim that crystal clouds significantly affect the radiation balance of the Earth-atmosphere system [1, 2]. However, the role of ice clouds in it is one of the least studied. Cirrus clouds can cause both greenhouse effect and cooling of the atmosphere. Various natural and technological processes (for example, seismic activity of the Earth bowels, increase or decrease in the temperature of the Arctic sea shelves, etc.) occurring on the land surface, in water, and on the water surface may change the structure of the atmosphere [3−5]. In this regard, monitoring of the composition of an aerodisperse medium can provide recording of these processes in hard-to-reach regions and-or under severe climatic conditions. The optical methods are considered to be the most effective ones for studying the aerodisperse media. They are based on the determination of the characteristics of radiation transformed by the propagation medium [6−9].

The ice clouds are characterized by a wide variety of particle shapes and sizes. Many factors (in particular, the temperature and humidity of the medium, air flow, position inside the cloud (in the middle or near the upper or lower cloud boundary), season, climatic zone, altitude, etc.) affect the microphysical properties of the atmospheric crystals [2, 10, 11]. Under definite conditions, those or other particle types with different effective sizes are formed. Thus, for example, Wolf *et al*. [12], based on numerous outdoor experiments, established that the average particle sizes varied from 10 to 1200 μm, and their concentrations changed from 3 to 400 L^{-1}. For smaller crystals, the observed concentration in some cases was higher by about two orders of magnitude. According to Shupe *et al*. [13], the average particle sizes characteristic of the Arctic troposphere, were the following: the effective ice crystal radius in winter was about 30 μm, and that of drops was 20 μm; in summer, these sizes increased by about 8 μm. In a formed ice cloud, the average crystal size can reach several hundred micrometers [2]. The largest crystals are localized in the lower part of the

[1]National Research Tomsk Polytechnic University, Tomsk, Russia, e-mail: shefer-ol@mail.ru; [2]National Research Tomsk State University, Tomsk, Russia, e-mail: vok44@mail.tsu.ru. Translated from Izvestiya Vysshikh Uchebnykh Zavedenii, Fizika, No. 12, pp. 105–113, December, 2021. Original article submitted March 11, 2021.

cloud. Under certain conditions (for example, at small water content above ice), crystals of regular extended shapes (for example, plates, or columns) are formed that often take a stable orientation in space.

Investigation of the influence of the shape, size, and concentration of particles, as well as of their optical properties and orientation, on the propagation of radiant energy is of paramount importance for understanding of the role of the ice clouds in the transformation of radiation fluxes and the determination of the nature of components comprised in aerosol media. Nowadays, the solution of the problem on radiant energy extinction by small (compared to the wavelength of propagating radiation) or large chaotically oriented particles is widely represented in the scientific literature [14−16]. Based on numerical and outdoor experiments on the determination of the optical characteristics of ice clouds, databases [17−20] have been created. They contain a large volume of data on the extinction characteristics of single crystals and their ensembles. At present, the problem of optical radiation transmission through an ensemble of translucent crystals with allowance for their spatial orientation and particle size distribution function remains urgent. This problem has been insufficiently studied for the propagation of infrared radiation.

Of greatest interest from the viewpoint of the nature of radiant energy transmission are particles responsible for the spectral dependence of the transmission function (TF). Among them are particles with sizes comparable to the incident radiation wavelength and large predominantly oriented crystals with plane parallel sides. For large particles without plane parallel sides, the radiant energy extinction is mainly determined by the diffraction field and is independent of the internal structure of a scatterer. Accordingly, the extinction efficiency factor takes the asymptotic value equal to 2. However, the extinction efficiency factor for other particles with sizes comparable to the radiation wavelength may differ significantly from this value. Small particles, as a rule, have chaotic orientation in space due to their aerodynamic properties [21]. When a polydisperse medium is considered, many light scattering features are smoothed.

In the present work, the transmission functions of chaotically and predominantly oriented crystals typical of the ice cloud are numerically investigated. As optical models, we consider: 1) particles of spherical shape, 2) mixtures of chaotically oriented crystals of different shapes, and 3) large predominantly oriented plates. The spherical particles are considered as an approximation model of chaotically oriented crystals disregarding their fine scattering structure caused by the feature of the scatterer shape. The examined mixture of crystals (particles and their aggregates, including hollow and solid columns and plates, droxtals, and bullet-shaped crystals) has allowed us to demonstrate the effect of the non-spherical particle shape on the character of the spectral dependence of light transmission. By the character of radiation extinction, plates are distinguished among all large predominantly oriented crystals. Their effective extinction factor can change in the range from 0 to 4 [22]. We have already presented the extinction characteristics estimated for large columns, plates, and crystals without plane-parallel sides in Ref. [23]. It was shown that among all large crystals, the plates provide the most clearly pronounced features and the stable behavior of the extinction characteristics attendant to changes in the physical and chemical particle parameters and radiation wavelengths. Based on results of outdoor experiments [2, 24, 25], it was reliably established that the crystal clouds include lamellar crystals.

The numerical ice cloud models used in this work have revealed the influence of the special features in the physical and chemical properties of atmospheric crystals on the behavior of the transmission function. In its turn, this has allowed us to establish the parameters of the medium at which this or that crystal type determines the spectral behavior of the transmission. When forming the model of the multicomponent medium, the possibility arises to justify the need for taking into account certain sizes and shapes of the particles.

FORMALISM

To calculate the transmission function (TF) for an ensemble of particles, the formula is valid

$$T = \exp(-\alpha_{ext} \cdot h). \quad (1)$$

Here h is the thickness of a homogeneous layer of the atmosphere. The extinction coefficient (α_{ext}) of the ensemble of particles, taking into account their size distribution function ($N(a)$) can be determined from the integral expression

$$\alpha_{\text{ext}} = \int S_{\text{ext}}(a) N(a)\, da\,, \tag{2}$$

where S_{ext} is the extinction cross section of a single particle. Here a is the particle size (for spheres and plates, it is equal to their radius; for particles of other shapes, it is equal to the effective particle size corresponding to their radius). The radius a and the thickness d of plates are related by the functional dependence $d = f(a)$, and r ($r = a/d$) is the form factor (or the aspect ratio of particle sizes). In the present work, we use

$$d = 2.020(2a)^{0.449}, \tag{3}$$

$$d = a/r, \tag{4}$$

obtained from the results of outdoor experiments [26, 27].

The range of cloud particle sizes (a) is determined by the modified γ-distribution with the clearly expressed modal value [27]. This distribution is described by the formula

$$N(a) = C \frac{\mu^{\mu+1}}{G(\mu+1)} \frac{1}{a_m} \left(\frac{a}{a_m}\right)^{\mu} \exp\left(\frac{-\mu a}{a_m}\right), \tag{5}$$

where a_m is the crystal size corresponding to the maximum of the function $N(a)$, μ is the dimensionless parameter characterizing the steepness of the slopes of this maximum (the variance-related parameter), and $G(\mu + 1)$ is the γ- function; the average particle size is calculated as $\overline{a} = a_m (1 + 1/\mu)$.

Various methods are used to determine numerically the extinction characteristics of particles. The method of dipole moments [28] and the T-matrix procedure [29] are widely used to calculate the characteristics of radiation scattering by non-spherical particles. However, their application is inefficient for particles whose sizes are much greater than the incident radiation wavelength. To calculate the characteristics of scattering by large crystals, the geometric optics method and its modification [30] are widely used. To take into account the vector nature of radiation, the most effective is the hybrid method representing a combination of geometric and physical optics [31] (in this context, it is often called *the method of physical optics*). For particles whose shape is close to a sphere, the Mie solution [32] of the problem of plane wave scattering by a sphere is used. Results of numerical investigations of the radiant energy extinction by the particles with sizes comparable to the incident radiation wavelength, many researchers indicated satisfactory agreement of the spectral dependence of the extinction by systems of spheres and ensembles of chaotically oriented crystals of different shapes [19, 33].

To calculate the extinction coefficient of a disperse medium, we used the optical models of ensembles of a) spherical particles, b) horizontally oriented hexagonal (round) plates, and c) mixtures of crystals having different shapes and internal structures (hollow or solid). The particle size distribution was described by the modified unimodal γ-distribution. The nature of the crystal material was characterized by the complex refractive index $\eta = n + i \cdot \chi$ (n is the real part of the refractive index and χ is its imaginary part). To calculate the spectral dependences of the optical characteristics, the spectral dependences $n = n(\lambda)$ and $\chi = \chi(\lambda)$ for pure ice [34] were used. In this work, we consider the wavelength range including visible, near-IR, and a part of mid-IR ranges, namely, from 0.5 to 15 μm. In this range, the complex refractive indices of water [35] and marine aerosol [36] differ slightly from the η values of ice (though impurities of different types may cause discrepancies). It is obvious that a natural atmospheric formation represents a mixture of a gas and particles, and the selectivity of the gas component may be manifested in a narrow spectral interval, for example, at high particle concentration. As a rule, in this case the dependence of the transmission on the wave number [37] was considered. For convenience of the subsequent estimation of the composition of a gas-disperse medium, the spectral dependence of the transmission function on the wave number is demonstrated in this paper.

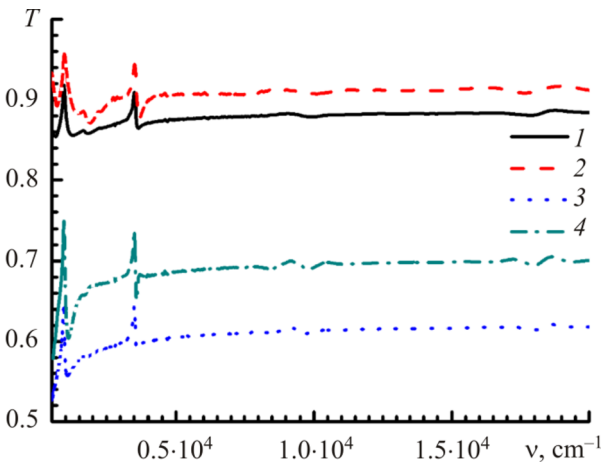

Fig. 1

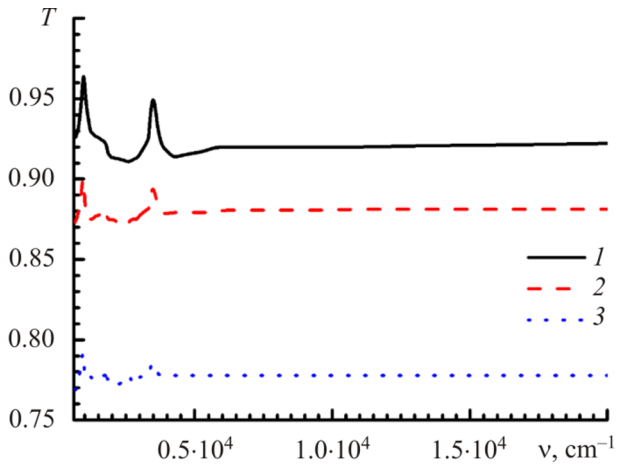

Fig. 2

Fig. 1. Spectral dependence of the transmission function $T(\nu)$ of the layer (h = 0.5 km) comprising spherical ice crystals for different parameters of the modified γ-distribution of particle sizes ($\overline{a}$ is the average radius, and μ characterizes the range of particle sizes) with the concentration C = 1000 L^{-1} and the complex refractive index of pure ice with $n = n(\nu)$ and $\chi = \chi(\nu)$ [34]. Here curve *1* is for $\overline{a}$ = 5 μm and μ = 1, curve *2* is for $\overline{a}$ = 5 μm and μ = 10, curve *3* is for $\overline{a}$ = 10 μm and μ = 1, and curve *4* is for $\overline{a}$ = 10 μm and μ = 10.

Fig. 2. Spectral dependence of the transmission function $T(\nu)$ of the layer (h = 0.5 km) comprising a mixture of ice crystals ($n = n(\nu)$ and $\chi = \chi(\nu)$ [34]) of different shapes and effective sizes $\overline{a}$. Here curve *1* is for $\overline{a}$ = 5 μm and C = 1000 L^{-1}, curve *2* is for $\overline{a}$ = 20 μm and C = 100 L^{-1}, and curve *3* is for $\overline{a}$ = 40 μm and C = 50 L^{-1}.

ANALYSIS OF CALCULATED RESULTS

To establish the main peculiarities of the optical radiation transmission function of the layer of a polydisperse ice medium, we consider crystals of different shapes and sizes that determine the spectral dependence of the extinction characteristics. We analyze the special features of the radiant energy transmission in the spectral range ν from 666.7 to 20 000 cm^{-1} that corresponds to the range of wavelengths λ from 15 to 0.5 μm (λ = 10000/ν). For definiteness, we consider the homogeneous layer of the medium with the thickness h = 0.5 km.

Figure 1 shows the calculated TF of optical radiation passed through the layer of the medium comprising spherical particles with the average size $\overline{a}$ = 5 μm (curves *1* and *2*) and $\overline{a}$ = 10 μm (curves *3* and *4*) for the indicated range of particle sizes. For the parameter μ = 1, the distribution $N(a)$ given by formula (5) is close to the uniform distribution, and for μ = 10, it has a clearly pronounced maximum. It should be noted that the distribution density functions $N(a)$ at μ = 5 and 10 differed slightly from each other (in comparison with the case of $N(a)$ for μ = 1 and 2). From Fig. 1 it can be seen that in the visible and near-IR spectral ranges, the neutral behavior of $T(\nu)$ is observed, except for small ranges where a weak dependence on ν is observed. In the mid-IR range for $\overline{a} \approx \lambda$, we observe the strongest dependence $T(\nu)$. Attention is drawn to the fact that the range of particle sizes for their identical average size has practically no effect on the shape of the $T(\nu)$ curves. The difference between $T(\nu)$ for μ = 1 and μ = 10 the greater, the larger is the average particle size. In this case, the special features in the spectral behavior of $T(\nu)$ are caused by the character of the dependence of the complex refractive index η(ν) for ice.

Let us consider the effect of the particle non-sphericity on the spectral behavior of the transmission function. Figure 2 shows the calculated TF for the layer of the medium comprising a mixture of chaotically oriented crystals,

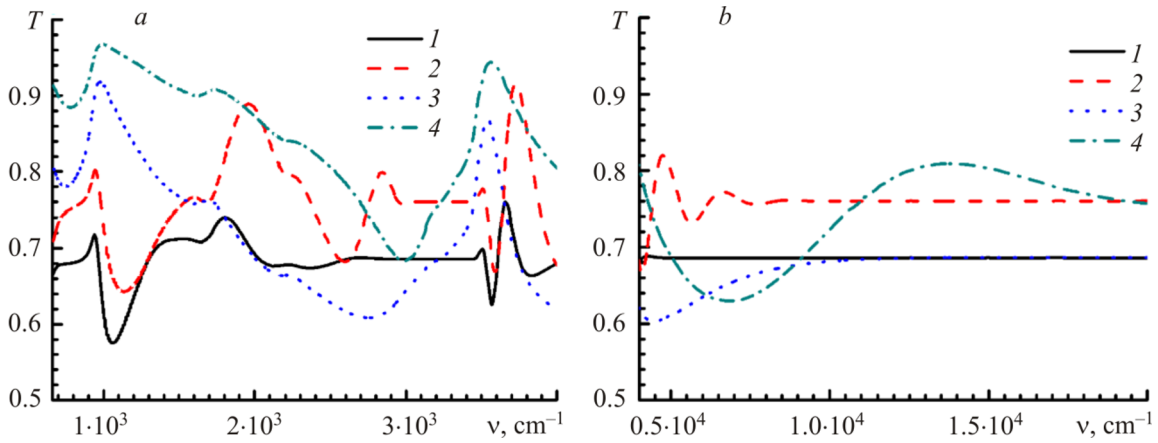

Fig. 3. Spectral dependence of the transmission function $T(\nu)$ of the layer (h = 0.5 km) of ice plates ($n = n(\nu)$ and $\chi = \chi(\nu)$ [34]) with the average size $\overline{a}$ = 40 μm and C = 50 L^{-1}. Here curve *1* is for μ = 1 and $d = 2.020(2a)^{0.449}$, curve *2* is for μ = 10 and $d = 2.020(2a)^{0.449}$, curve *3* is for μ = 1 and a/d = 20, curve *4* is for μ = 10 and a/d = 20; ν = [660 cm^{-1}, $4\cdot10^3$ cm^{-1}] (*a*) and ν = [$4\cdot10^3$ cm^{-1}, $2\cdot10^4$ cm^{-1}] (*b*).

including droxtiles, plates, hollow and solid columns, and bullet-shaped rosettes of crystals as well as aggregates of dense columns and plates. The dependences $T(\nu)$ shown in Fig. 2 were obtained using the database [17] of the optical characteristics of cloud crystals. For calculations, the method of dipole moments, the T-matrix technique, and the improved method of geometric optics were used. Based on the calculated results, we have established that the effect of the range of particle sizes is negligibly small. The most clearly pronounced dependence $T(\nu)$ was observed when the wavelength was comparable to the effective particle size. Compare curve *1* in Fig. 2 and curve *2* in Fig. 1 for particles with the same sizes ($\overline{a}$ = 5 μm). The differences were observed only in the fine structure of $T(\nu)$ in the wavelength ranges of two clearly pronounced maxima that corresponded to the positions of the main minima of $n(\nu)$ (n(920 cm^{-1}) ≈ 1.083 and n(3440 cm^{-1}) ≈ 0.955). The larger the particle, the weaker was the spectral dependence of the transmission. In the wavelength ranges where $\overline{a} >> \lambda$, we observed the neutral behavior; in this case, the TF reached its asymptotic values; at the same time, the effective extinction factor was equal to 2.

As already indicated above, the predominantly oriented plates can be distinguished among all large crystals by the character of their extinction. Figures 3, 4, and 6 show numerical values of the transmission function for horizontally oriented ice plates obtained by the method of physical optics. For this crystal shape, the spectral dependence in the optical wavelength range is most clearly pronounced. Figure 3 shows the calculated TF for plates with the average size $\overline{a}$ = 40 μm and the indicated μ values and the aspect ratio r. For the plates, values of these parameters affect significantly the behavior of $T(\nu)$. If we compare curves *1* and *2* or *3* and *4* in Fig. 3, it becomes clear that the larger the range of particle sizes (μ = 1), the smoother the dependence $T(\nu)$. Curves *1* and *2* show the TF for $d = f(a)$ given by Eq. (3), and curves *3* and *4* – for d given by Eq. (4) at r = 20. Thus, the neutral behavior of $T(\nu)$ is observed in the visible and near-IR ranges for relatively thick plates (according to Eq. (3), $\overline{a}/\overline{d}$ = 14.45 for $\overline{a}$ = 40 μm) for a wide range of particle sizes. For relatively thin plates (r = 20) with relatively narrow range of their sizes (μ = 10), the spectral dependence of the TF can be seen even in the visible range of wavelengths. Comparing the characters of the dependence $T(\nu)$ for non-spherical particles with the same sizes (curve *4* in Fig. 2 for $\overline{a}$ = 40 μm and curves *1*–*4* in Fig. 3), we see the obvious difference between the TF for chaotically oriented crystals and horizontally oriented plates. Positions of the maxima of $T(\nu)$ caused by the clearly pronounced minima of $n(\nu)$ (indicated above when discussing Fig. 2) are slightly shifted, but their amplitudes differ significantly for relatively thick and thin plates. Such special features are not peculiar to spheres or chaotically oriented crystals. The limits of variations of the TF for optical radiation increased with the particle size variance and the aspect ratio.

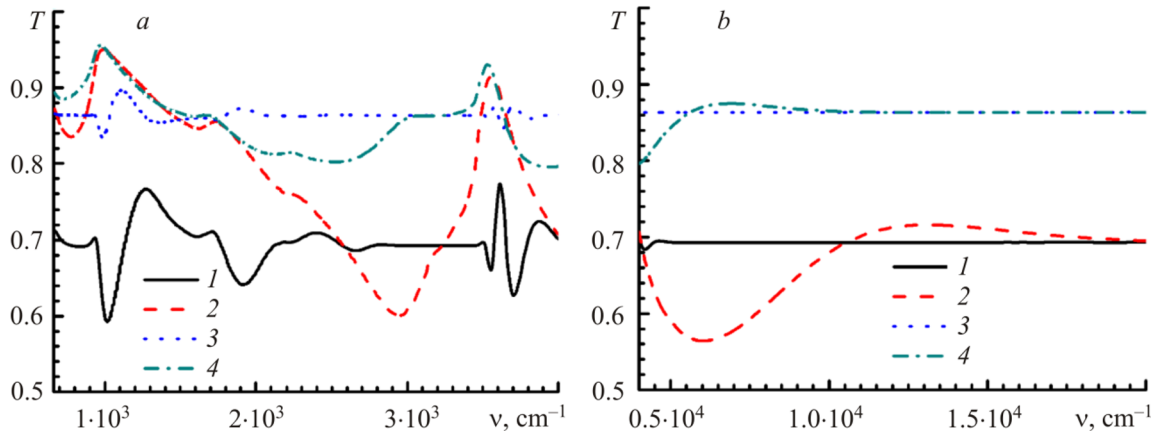

Fig. 4. Spectral dependence of the transmission function $T(\nu)$ of the layer (h = 0.5 km) comprising ice plates ($n = n(\nu)$ and $\chi = \chi(\nu)$ [34]) with different average sizes $\overline{a}$ and $\mu = 5$. Here curve *1* is for $\overline{a}$ = 100 μm, $d = 2.020(2a)^{0.449}$, and $C = 10$ L^{-1}; curve *2* is for $\overline{a}$ = 100 μm, $a/d = 20$, and $C = 10$ L^{-1}; curve *3* is for $\overline{a}$ = 200 μm, $d = 2.020(2a)^{0.449}$, and $C = 1$ L^{-1}; curve *4* is for $\overline{a}$ = 200 μm, $a/d = 20$, and $C = 1$ L^{-1}; $\nu = [660\ \text{cm}^{-1}, 4\cdot10^3\ \text{cm}^{-1}]$ (*a*) and $\nu = [4\cdot10^3\ \text{cm}^{-1}, 2\cdot10^4\ \text{cm}^{-1}]$ (*b*).

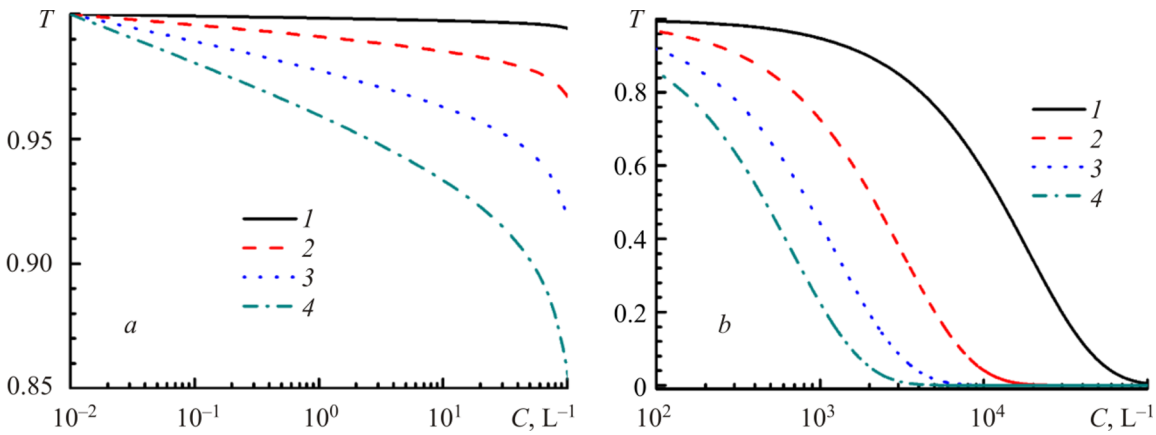

Fig. 5. Transmission function $T(C)$ of the layer (h = 0.5 km) depending on the concentration of spherical ice particles ($n = n(\nu)$ and $\chi = \chi(\nu)$ [34]) with different average sizes, $\mu = 5$, and $\lambda = 10.6$ μm ($\nu = 943.4$ cm^{-1}). Here curve *1* is for $\overline{a}$ = 5 μm, curve *2* is for $\overline{a}$ = 10 μm, curve *3* is for $\overline{a}$ = 15 μm, and curve *4* is for $\overline{a}$ = 20 μm; $C = [10^{-2}\ \text{L}^{-1}, 10^2\ \text{L}^{-1}]$ (*a*) and $C = [10^2\ \text{L}^{-1}, 10^5\ \text{L}^{-1}]$ (*b*).

Figure 4 shows the dependences $T(\nu)$ calculated for plates with different aspect ratios and different average sizes, but with the same variance. In the mid-IR range, the behavior of $T(\nu)$ differed significantly when the average geometric sizes of plates changed. The most clearly pronounced spectral dependence of the TF was observed for plates with smaller sizes and larger aspect ratios (compare curve *2* with curves *1*, *3*, or *4* in Fig. 4).

It is well known that natural predominantly oriented systems of particles oscillate about their stable equilibrium positions in space. Based on our previous numerical estimations [22, 23], we established that the flutter of plates insignificantly affected the radiation extinction and caused no radical changes in the dependences of the characteristics at small deflection angles of ice plates (less than about 20°). The special features (the positions of the minima and maxima in the spectral behavior of the optical characteristic) remained unchanged.

Figure 5 (for spheres) and Fig. 6 (for plates) show the dependences of the transmission function on the concentration of particles with different average sizes at the wavelength $\lambda = 10.6$ μm ($\nu = 943.392$ cm^{-1}). Numerical

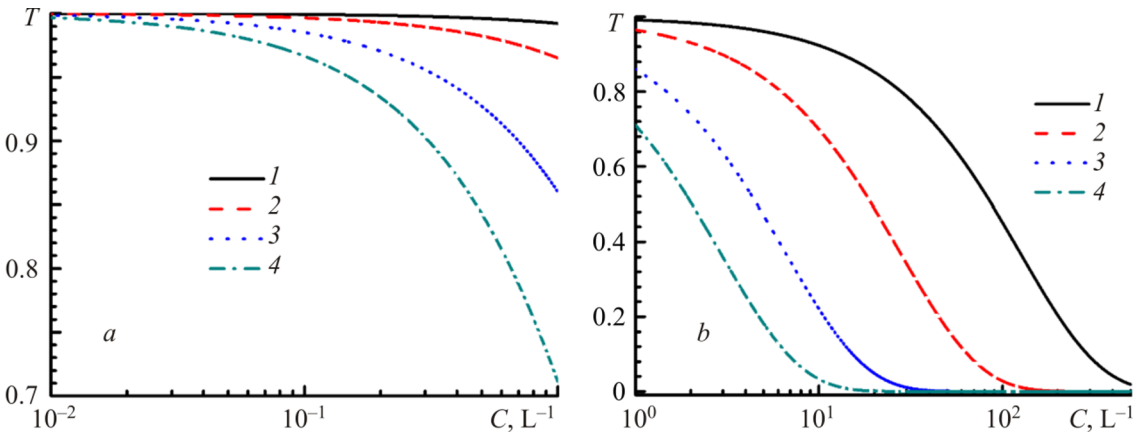

Fig. 6. Transmission function $T(C)$ of the layer (h = 0.5 km) of ice plates ($n = n(\nu)$ and $\chi = \chi(\nu)$ [34]) with different average sizes, $\mu = 5$, and $\lambda = 10.6$ μm ($\nu = 943.4$ cm^{-1}). Here curve *1* is for $\overline{a} = 50$ μm, curve *2* is for $\overline{a} = 100$ μm, curve *3* is for $\overline{a} = 200$ μm, and curve *4* is for $\overline{a} = 300$ μm; $C = [10^{-2}$ L^{-1}, 1 L$^{-1}]$ (*a*) and $C = [1$ L^{-1}, $5 \cdot 10^2$ L$^{-1}]$ (*b*).

values of $T(C)$ can be used to estimate the absolute values of the TF depending on the average particle sizes and their concentrations per unit volume.

Thus, the general character of the spectral dependence of the TF is primarily determined by the interrelation between the refractive index of the particle material and the radiation wavelengths. The particle shapes and average sizes, as well as the character of particle orientation in space, introduce second-order corrections to the behavior of the transmission function. All these factors should be taken into account when estimating the TF data. The problem is simplified when the microphysical characteristics of the examined medium are known *a priori*, at least approximately.

CONCLUSIONS

The polydisperse medium was modeled here by an ensemble of crystals important from the viewpoint of the spectral behavior of radiation transmission. Among these crystals, the scatterers with sizes comparable to the radiation wavelength and large predominantly oriented crystals, including plates that predominantly affected the spectral behavior of the extinction characteristics, can be distinguished.

It has been shown that the clearly pronounced special features of the TF for particles whose sizes are comparable to the incident radiation wavelength were primarily caused by the particle material and the functional relationship between the particle refractive index and the radiation wavelength. The shapes and the average sizes of such crystals lead only to different thin structure of the spectral behavior of the transmission function. The variance of the particle sizes affected mostly the spectral position of the asymptotic limit of the transmission function ($T(\nu) = \text{const}$). Investigation of the thin structure of this optical characteristic for relatively small crystals requires additional consideration with allowance for the specific application field focused on a single crystal or a polydisperse medium.

On the example of the ensemble of large horizontally oriented plates, it was shown that the special features in the spectral behavior of the transmission function were more pronounced in the mid-IR range (as for the particles whose sizes were compared to the radiation wavelength). The average sizes of plates, their variance, aspect ratio, and certainly, the dependence of the refractive index on the wavelength – all these parameters significantly affected the character of the spectral behavior of the TF. For thin plates, the clearly pronounced spectral dependence of the transmission function was observed even in the near-IR and visible ranges. Taking into account of this special feature is the important factor in determining spectral ranges in which the selectivity of some components of the gas-disperse medium is manifested. The variance of the particle sizes and the aspect ratio of particles affect the formation of clearly pronounced special

features in the behavior of the TF which differs significantly even for the same average particles sizes in the mid-IR range (in particular, from 600 cm^{-1} to $5 \cdot 10^3$ cm^{-1}).

The calculated transmission functions presented in this work for spheres and plates depending on the concentration of particles of different average sizes per unit volume allow the transmittance of the medium with the preset microphysical parameters to be evaluated at required wavelengths. For the same concentrations of particles typical for most crystal clouds, the greatest contribution to the formation of the special features in the spectral dependence of the transmission function was provided by large predominantly oriented plates.

Traditionally, large atmospheric crystals are associated with neutral behavior of the radiant energy transmission function. This was justified for chaotically oriented particles. Results of outdoor experiments showed that ensembles of predominantly oriented lamellar crystals were often encountered in ice clouds. Results of numerical investigation of the spectral dependence of the transmission function for large plates presented in this work significantly complement the existing knowledge. The neglect of the special features of the optical radiation transmission function for lamellar crystals may cause both small errors (in the visible and near-IR ranges for thick plates with a wide range of their sizes) and drastically wrong estimates (in the presence of thin plates).

The results of numerical investigation of the transmission function of optical radiation for different particle models were put in correspondence with the physical and chemical parameters of the propagation medium and the radiation characteristics. This has allowed us to compare correctly and to estimate the effect of different components of the medium on the radiant energy propagation. The conclusions obtained are new and relevant for multicomponent aerodisperse media. Results of numerical investigation of the optical characteristic of the medium are presented depending on the wave number, which is traditional for the gaseous component. Such representation is important for practical applications, because it provides direct data matching when analyzing the TF of a gas and aerosol mixture.

To investigate the fine structure of the spectral dependence of ice cloud extinction characteristics, particles with different physical and chemical properties should be considered. Such problem is practically unsolvable because of huge variety of particles. In this work, the general peculiarities have been revealed and the stable optical effects manifested in the process of interaction of radiant energy with atmospheric crystals have been established for different spectral ranges.

This research was supported by National Research Tomsk Polytechnic University Development Program and the Program of Increasing the Competitiveness of National Research Tomsk State University among Leading International Research and Education Centers.

REFERENCES

1. T. F. Stocker, D. Qin, G.-K. Plattner, *et al*., eds., IPCC. Climate Change 2013: The Physical Science Basis. Contribution of Working Group I to the Fifth Assessment Report of the Intergovernmental Panel on Climate Change, Cambridge University Press, Cambridge; New York (2013).
2. A. Baran, Atm. Res., **112**, 45–69 (2012).
3. A. I. Obzhirov, Yu. A. Telegin, and A. V. Boloban, Underwater Investigations and Robotics, No. 1, 56–63 (2015).
4. B. Croft, G. R. Wentworth, R. V. Martin, *et al*., Nature Commun., **15**, No. 7, 13444 (2016); DOI: 10.1038/ncomms13444/.
5. G. Guyot, F. Olofson, P. Tunved, *et al*., Atmos. Chem. Phys. Discuss., 1–28 (2017); DOI: 10.5194/acp-2017-672.
6. E. D. Hinckley, Laser Monitoring of the Atmosphere [Russian translation], Mir, Moscow (1976).
7. V. A. Arkhipov, I. R. Akhmadeev, S. S. Bondarchuk, *et al*., Opt. Atm. Okeana, **20**, No. 1, 48–52 (2007).
8. S. J. Cooper and T. J. Garrett, Atmos. Meas. Tech., **4**, 1593–1602 (2011).
9. M. D. Alexandrov and M. I. Mishchenko, Opt. Express, **25**, No. 4, A134–A150 (2017); DOI: 10.1364/OE.25.00A134.
10. M. Koike, J. Ukita, J. Ström, *et al*., GDR Atmospheres, 1798−1822 (2019); DOI: 10.1029/2018JD029802.

11. G. Moiche, O. Jourdan, J. Delanoë, *et al*., J. Atmos. Chem. Phys., **17**, 12845–12869 (2017); DOI: 10.5194/acp-17-12845-2017.
12. V. Wolf, T. Kuhn, M. Milz, *et al*., Atmos. Chem. Phys., **18**, 17371–17386 (2018); DOI: 10.5194/acp-18-17371-2018.
13. M. D. Shupe, D. D. Turner, A. Zwink, *et al*., J. Appl. Meteorol. Climat., **54**, 1675–1689 (2015); DOI: 10.1175/JAMC-D-15-0054.1.
14. A. J. Baran, J. Quant. Spectrosc. Radiat. Transfer, **110**, 1239–1260 (2015).
15. H. Moosmüller and C. M. Sorensen, J. Quant. Spectrosc. Radiat. Transfer, **204**, 250–255 (2018).
16. H. Moosmüller and C. M. Sorensen, J. Quant. Spectrosc. Radiat. Transfer, **219**, 333–338 (2018).
17. B. Baum, P. Yang, A. Heymsfield, *et al*., J. Quant. Spectrosc. Radiat. Transfer, **146**, 123−139 (2014).
18. P. Yang, L. Bi, B. Baum, *et al*., Atm. Sci., **70**, 330–347 (2013); DOI: 10.1175/JAS-D-12-039.1.
19. C. Schmitt, M. Schnaiter, A. Heymsfield, *et al*., Atm. Sci., **73**, 4775–4791 (2016); DOI: 10.1175/JAS-D-16-0126.1.
20. L. Bi and P. Yang, J. Quant. Spectrosc. Radiat. Transfer, **189**, 228–237 (2017); DOI: 10.1016/j.jqsrt.2016.12.007.
21. J. Giovacchini, Q. J. R. Meteorol. Soc., **143**, 3085–3093 (2017); DOI: 10.1002/qj.3164.
22. O. V. Shefer, J. Quant. Spectrosc. Radiat. Transfer, **117**, 104–113 (2013).
23. O. V. Shefer, J. Quant. Spectrosc. Radiat. Transfer, **178**, 350–360 (2016).
24. C. Zhou, P. Yang, A. Dessler, and F. Liang, IEEE Geosci. Remote Sensing Lett., **10**, 986–990 (2013).
25. S. Platnick, K. Meyer, M. King, *et al*., Trans. Geosci. Remote Sensing, **55**, 502–525 (2017).
26. P. Yang and Q. Fu, J. Quant. Spectrosc. Radiat. Transfer, **110**, 1604–1614 (2009).
27. O. A. Volkovitskii, L. N. Pavlova, and A. G. Petrushin, Optical Properties of Crystal Clouds, Gidrometeoizdat, Leningrad (1984).
28. M. A. Yurkin and A. G. Hoekstra, J. Quant. Spectrosc. Radiat. Transfer, **112**, 2234–2247 (2011).
29. M. I. Mishchenko, N. T. Zakharova, N. G. Khlebtsov, *et al*., J. Quant. Spectrosc. Radiat. Transfer, **178**, 276–283 (2016).
30. L. Bi, P. Yang, G. W. Kattawar, *et al*., J. Quant. Spectrosc. Radiat. Transfer, **112**, 1492–1508 (2011).
31. A. A. Popov, Proc. SPIE, **2822**, 186–194 (1996).
32. K. Boren and D. Hafman, Absorption and Scattering of Light by Small Particles [Russian translation], Mir, Moscow (1986).
33. H. Iwabuchi, S. Yamada, and S. Katagiri, Appl. Met. Climat., **53**, 1297–1316 (2014); DOI: 10.1175/JAMC-D-13-0215.1.
34. S. G. Warren and R. E. Brandt, J. Geophys. Res., **113**, D14220 (1–10) (2008).
35. H. D. Downing and D. Williams, J. Geophys. Res., **80**, No. 12, 1656–1661 (1975).
36. R. Irshad, R. G. Graindger, D. M. Peters, *et al*., Atmos. Chem. Phys., **9**, 221–230 (2009).
37. O. K. Voitsekhovskaya, D. E. Kashirskii, O. V. Egorov, and O. V. Shefer, J. Appl. Opt., **55**, 3814–3823 (2016); DOI: 10.1364/AO.55.003814.